# RECONSTRUCTION OF SUBSTANCE FROM SHADOW*

## I. Mathematical Theory with Application to Three-Dimensional Radiography and Electron Microscopy

By G. N. Ramachandran

(*Department of Biophysics, University of Chicago, Chicago, Illinois* 60637)

*and*

(*Molecular Biophysics Unit, Indian Institute of Science, Bangalore*-12, *India*)

Received February 27, 1971

I. *Mathematical principle of integrograph reconstruction.*—If $f(x, y)$ represents the areal density distribution of a finite lamellar object (Fig. 1) and $|f(x, y)|$ has an upper bound, then it can be represented in terms of its Fourier transform F (X, Y) according to Eqs. (1) and (2)

$$f(x, y) = \int_{-\infty}^{+\infty} \int_{-\infty}^{+\infty} \mathrm{F}(\mathrm{X}, \mathrm{Y}) \exp[-2\pi i(x\mathrm{X} + y\mathrm{Y})]\, d\mathrm{X}\, d\mathrm{Y}, \qquad (1)$$

where

$$\mathrm{F}(\mathrm{X}, \mathrm{Y}) = \int_{-\infty}^{+\infty} \int_{-\infty}^{+\infty} f(x, y) \exp[2\pi i(x\mathrm{X} + y\mathrm{Y})]\, dx\, dy. \qquad (2)$$

Equation (1) can also be expressed in polar coordinates, symbolized in Fig. 1, in the form

$$f(r, \phi) = \int_{0}^{+\infty} \int_{0}^{2\pi} \mathrm{F}(\mathrm{R}, \Phi) \exp[-2\pi i \mathrm{R} r \cos(\phi - \Phi)]\, \mathrm{R}\, d\mathrm{R}\, d\Phi. \qquad (3)$$

Also, integrating (1) over $y$, we have, for the projected linear density along the $x$-axis,

$$\int_{-\infty}^{+\infty} f(x, y)\, dy = g(x)$$

$$= \int_{-\infty}^{+\infty} \int_{-\infty}^{+\infty} \mathrm{F}(\mathrm{X}, \mathrm{Y}) [\exp(-2\pi i x\mathrm{X})] \times \left[\int_{-\infty}^{+\infty} \exp(-2\pi i y\mathrm{Y})\, dy\right] d\mathrm{X}\, d\mathrm{Y}. \qquad (4)$$

* Thanks are due to the U.S. Public Health Service, Grant No. AM 11493, and the Jane Coffin Childs Memorial Foundation for grants which made this investigation possible. I am also grateful to Dr. A. V. Lakshminarayanan for assistance in the work described in Section V, and to Dr. Raghavan Narasimhan for discussions on the Paley-Wiener theorem mentioned in Section VII. Thanks are also due to Mr. J. Hansley of the Institute for Computer Research for preparing the programmes for obtaining Figs. 5 (*a*) and (*b*).

Now $\int_{-\infty}^{+\infty} \exp(-2\pi i y\mathrm{Y})\, dy = \delta(\mathrm{Y}-0)$[1], so that (4) becomes

$$g(x) = \int_{-\infty}^{+\infty} \mathrm{F}(\mathrm{X},0)\, \exp(-2\pi i x\mathrm{X})\, d\mathrm{X}. \tag{5}$$

Inverting this Fourier transform, we also have

$$\mathrm{F}(\mathrm{X},0) = \int_{-\infty}^{+\infty} g(x)\, \exp(2\pi i x\mathrm{X})\, dx. \tag{6}$$

It is obvious that the line $\mathrm{Y}=0$ in reciprocal space corresponds also to $\Phi = 0$ and R going from $-\infty$ to $+\infty$, so that

$$\mathrm{F}(\mathrm{X},0) = \mathrm{F}(\mathrm{R},0),\ \mathrm{X}=0 \text{ to } +\infty,\ \mathrm{R}=0 \text{ to } \infty, \tag{7 a}$$

$$\mathrm{F}(\mathrm{X},0) = \mathrm{F}(\mathrm{R},\pi),\ \mathrm{X}=0 \text{ to } -\infty,\ \mathrm{R}=0 \text{ to } \infty. \tag{7 b}$$

f we rotate both the real and reciprocal axes of coordinates in Fig. 1 by an angle $\theta$ (Fig. 2 *a*) so that

$$\begin{aligned}(x', \mathrm{X}') &= (x, \mathrm{X})\cos\theta + (y, \mathrm{Y})\sin\theta \\ (y', \mathrm{Y}') &= -(x, \mathrm{X})\sin\theta + (y, \mathrm{Y})\cos\theta\end{aligned} \tag{8}$$

and define

$$g(x') = \int_{-\infty}^{+\infty} f(x', y')\, dy', \tag{9}$$

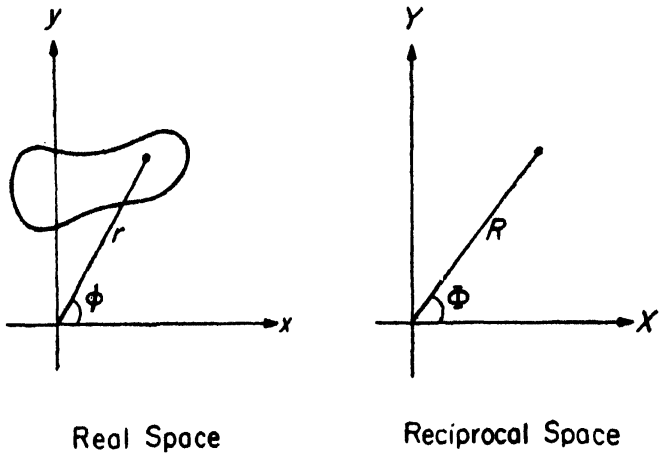


FIG. 1. Coordinate axes in real and imaginary space.

then it follows that

$$F(x', 0) = \int_{-\infty}^{+\infty} g(x') \exp(2\pi i x' X') \, dx'. \tag{10}$$

Since

$$F(X', 0) = F(R, \theta), \; X' = -\infty \text{ to } +\infty, \; R = -\infty \text{ to } +\infty, \tag{11}$$

which is the same as $F(R, \theta)$, $R = 0$ to $+\infty$ and $F(R, \theta + \pi)$, $R = 0$ to $+\infty$, we thus find that the complete $F(R, \Phi)$ of the object can be determined, if we know $g(x')$ over the region $-\infty < x' < +\infty$, for a range of values of $\theta$ going from 0 to $\pi$, and hence $f(r, \phi)$ can be reconstructed. The final formulae may therefore be written explicitly as follows:

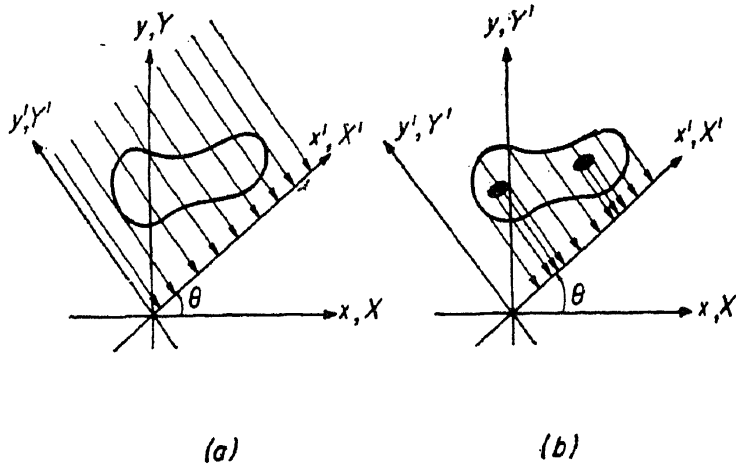


FIG. 2 (*a*) Formation of shadowgraph (or integrograph) at angle $\theta$. (*b*) Formation of collimated autoradiograph at angle $\theta$.

The function $g(x')$, which is the same as $g(r; \theta)$ † for $-\infty < r < +\infty$ and constant $\theta$, may be called the integrograph of $f(x, y)$ for the orientation $\theta$. It is obtained by integrating the function along lines perpendicular to the line $\phi = \theta$. If we physically determine $g(r; \theta)$ over the ranges $-\infty < r < \infty$ and $0^- \leq \theta < \pi$, then the two-dimensional function $f(r, \phi)$ can be reconstructed by the following process:

† A semicolon is used between $r$ and $\theta$ in $g(r;\theta)$ to indicate that the physically important variable is $r$, while $\theta$ is a fixed parameter. However, $\theta$ also becomes a variable in going from Eq. (12) to Eq. (13).

(*a*) Obtain the one-dimensional Fourier transform of $g(r;\theta)$ given by

$$F(R,\theta) = \int_{-\infty}^{+\infty} g(r;\theta) \exp(2\pi i r R)\, dr \tag{12}$$

for $-\infty < R < \infty$, which yields $F(R,\theta)$ and $F(R,\theta+\pi)$, for $R=0$ to $+\infty$.

(*b*) Calculate the two-dimensional Fourier transform of the function $F(R,\theta)$ $[0 \leq R < \infty,\ 0 \leq \theta \leq \pi]$ to obtain $f(r,\phi)$ as

$$f(r,\phi) = \int_0^{+\infty} \int_0^{2\pi} F(R,\theta) \exp[-2\pi i R r \cos(\phi-\theta)]\, R\, dR\, d\theta. \tag{13}$$

II. *Three-dimensional shadowgraph reconstruction.*—Equations (12) and (13) contain the principle of the method of obtaining the *three*-dimensional density distribution of an object from measurements made on its shadows in various directions. Taking the two-dimensional example, if radiation is incident along the direction $y'$, then the intensity distribution along $x'$ is

$$I(x') = I_0 \exp\left[-\int_{-\infty}^{+\infty} \mu(x',y')\,\rho(x',y')\, dy'\right] \tag{14}$$

or

$$\log I_0 - \log I(x') = g(x') = \int_{-\infty}^{+\infty} f(x',y')\, dy' \tag{15}$$

where $f(x',y') = \mu(x',y')\,\rho(x',y')$ is the relevant function, whose integral can be determined experimentally. In this, $\rho$ is the density, and $\mu$ the analogue of the mass absorption coefficient, for the radiation, and $\mu$ may be termed the "optical density" of the material. Since Eq. (15) has the same form as Eq. (9), it is possible to reconstruct $f(x,y)$ $[\equiv f(r,\theta)]$ from measurements made on shadowgraphs taken at different inclinations $\theta$.

The extension to three dimensions is obvious. The best method appears to consist in rotating the three-dimensional object about an axis (say the $z$-axis) through angles $\theta$ and taking shadowgraphs for different values of $\theta$. If cylindrical polar coordinates $(r,\phi,z)$ and $(R,\Phi,Z)$ are taken for the real and reciprocal axes, then Eqs. (12) and (13) are completely valid, in the more generalized form

$$F(R,\theta:z) = \int_{-\infty}^{+\infty} g(r;\theta;z) \exp(2\pi i r R)\, dr,$$

$$0 \leq \theta \leq \pi;\quad -\infty < z < \infty;\quad -\infty < R,\ r < \infty \tag{16}$$

and

$$f(r, \theta, z) = \int_0^{+\infty} \int_0^{\pi_2} F(R, \theta; z) \exp\ [-2\pi i R r \cos(\phi - \theta)]\, R\, dR\, d\theta, \tag{17}$$

noting that $F(R, \theta; z) = F(|R|, \theta + \pi; z)$ if R is negative. In other words, one can reconstruct a series of sections for each $z$, exactly as in the two-dimensional case. (Semicolons are used for parameters, as above.)

The physical significance of Eqs. (16) and (17) may be stated as follows:

The object (Fig. 3) is rotated about the $z$-axis and the shadowgraph at an angular setting $\theta$ may be considered to be a superposition of a series of shadows of thin sections at right angles to the $z$-axis. In the limit, each of these sections, at distance $z$ from origin, gives a linear shadow along the $x'$-axis, so that the problem reduces to the reconstruction of a series of two-dimensional planar sections from the set of linear shadowgraphs for each section. In other words, the Fourier transformation, *via* the reciprocal space, and reconstruction are carried out only for the variables $r$ and $\theta$. The variable $z$ is in real space, and the reconstruction can be made section by section, and they could then be put together. The computations required are only for the series of one-dimensional Fourier transforms of each linear shadow at $\theta$ and the two-dimensional back-transform for the reconstruction of each place. Thereafter, the reconstructed images can be stored in digital form in serial order of $z$ and can be recalled in any manner that is needed.

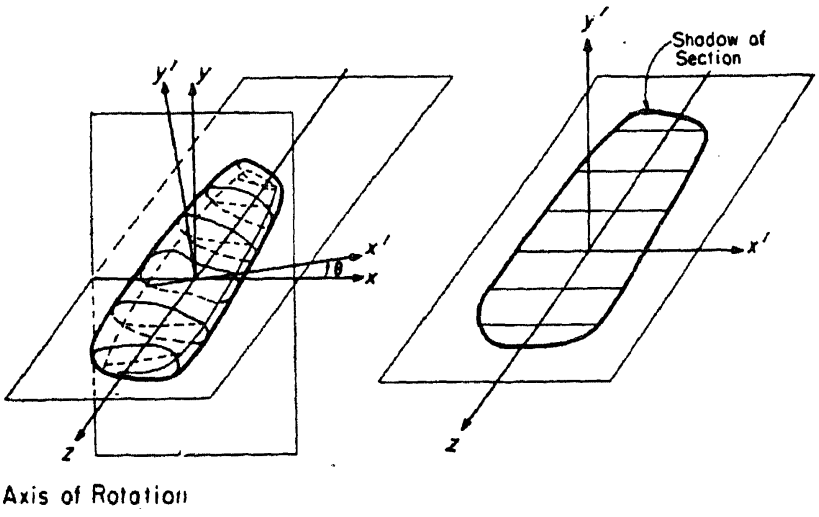


FIG. 3. Formation of shadowgraph from lamellar sections normal to the axis of rotation.

It is also possible to take shadowgraphs by rotating the object not only about one axis, but more generally in various orientations in space. In this way, data are obtained for the Fourier transform $F(R, \Phi, Z)$. These can then be utilized to make a three-dimensional Fourier transform of the form

$$f(r, \phi, z) = \int_{-\infty}^{+\infty} \int_{0}^{\pi} \int_{-\infty}^{+\infty} F(R, \Phi, Z) \exp\ [-2\pi i \{Zz + Rr \cos(\phi - \Phi)\}]. \times R\, dR\, d\Phi\, dZ. \quad (18)$$

If data are obtained by making incomplete rotations about different axes, then it may still be possible to obtain one complete set required for the reconstruction.

III. *Practical applications.*—This technique of reconstruction from shadowgraphs has great potentiality in practical applications. For instance, it can be used for the location and analysis of tumours deep inside the body by radiography. Even the exact shape and texture of the tumour can be "seen" by digitising the data on the radiograph by television-screen scanning techniques and then reconstructing the three-dimensional structure either digitally, or in the form of sections photographically, or on a cathode ray screen, which can be viewed either as a whole, or in sections. By using special elements like iodine which tend to concentrate in some tumours, the process can be intensified.

The shadowgraph technique can also be used in electron microscopy—for instance to get a full three-dimensional picture of a cell. The use of high voltage electron beams makes this method particularly suitable for this purpose. H. Fernandez-Moran[2,3] has developed high voltage electron voltage electron microscopes with superconducting lenses which go to molecular resolution. Again, if techniques are available whereby the effects of regions having particular elements are intensified, the location of such regions can be pinpointed. Dr. A. V. Crewe in the University of Chicago has developed such techniques using a scanning electron microscope, which also go to high resolution, close to atomic dimensions.[4,5] This makes it possible even to *see* the three-dimensional structure of large molecules like proteins and nucleic acids. The use of heavy atom markers would be valuable for this purpose for pinpointing reference locations. Thus, direct electron microscopy can be used to supplement X-ray diffraction as a means of three-dimensional structure analysis. It is gratifying that this technique also has as its basis the method of Fourier transforma-

tion. On the other hand, there is no 'phase problem', as in orthodox crystallography.

In technology, the radiographic technique can be used even more as a tool than before. Instead of having to guess at the nature and shape of defects from shadowgraphs at different angles, they can actually be reconstructed in three dimensions.

In all these applications, one of the most important of the practical aspects is the cross-correlation of different shadowgraphs such that the shadow of the axis of rotation is exactly coincident in every one of them used in the analysis. This is in a way analogous to the phase problem in crystallography. In the case of gross objects, this poses no problem, for the shadow of an opaque wire kept along the axis can be obtained in each picture. Some method of overcoming this problem has to be devised in electron microscopy. If the rotation technique is employed, then the existence of one reference point (which has either a high positive or negative contrast) is sufficient; in the general case, three reference points are needed to fix the orientation. The question of resolution in relation to the number of shadowgraphs to be recorded and the effect of the absence of data for certain ranges of $\theta$ have to be investigated.

In emphasizing the use of the shadowgraph, we have implicitly assumed that the function $f(x, y)$ or $f(x, y, z)$ is real. This is not necessary for the general validity of the mathematical theorems stated above for integrograph reconstruction. Equations (12) and (13), with the definition (9) for $g(r; \theta)$, are true for any function $f(x, y)$ which has a Fourier transform.

IV. *Method for point-source shadowgraphs.*—While Fig. 2, in which the shadowgraph is recorded by a parallel beam, is valid for the application to electron microscopy, a divergent beam from a point source, as in Fig. 4, is used in radiography. However, it is easy to see that the shadowgraphs obtained in this case contain the information to obtain the true $g(r; \theta)$ corresponding to the parallel beam case, but in a scrambled manner. This is seen from Fig. 4, in which S is the point source and the shadowgraph is recorded in a plane perpendicular to the line SO, passing through the axis of rotation. Analogous to Fig. 2, we denote by $Ox''$, $Oy''$ the rotated axes, at setting $\theta''$, with $Oy''$ lying along OS (of length L) directed from the origin to the source. For convenience, we shall consider the shadowgraph plane to pass through the axis, *i.e.*, along $Ox''$. (In actual practice, this requires only a scaling.)

If we represent by $h(r''; \theta'')$ the shadowgraph function along $Ox''$, it is clear that this is cast by the ray SP″, where the length OP″ $= r''$. Now if OP′ is drawn normal to SP″, then it is clear that we may associate the point P″ in the point shadowgraph at $\theta''$, with the point P′ in a plane at angle $\theta$ to the direction $Ox$. However, if such an association is made for each $r''$ at $\theta''$, then both $r'$ and $\theta$ will be different for each case, with only the common property that, for every one of the associated points P′, the ray will be normal to the corresponding $Ox'$. Thus, it is obvious that parallel beam shadowgraph data can be obtained from the point source shadowgraphs, using the following unscrambling function:

$$g(r'; \theta) = h(r''; \theta''), \tag{19}$$

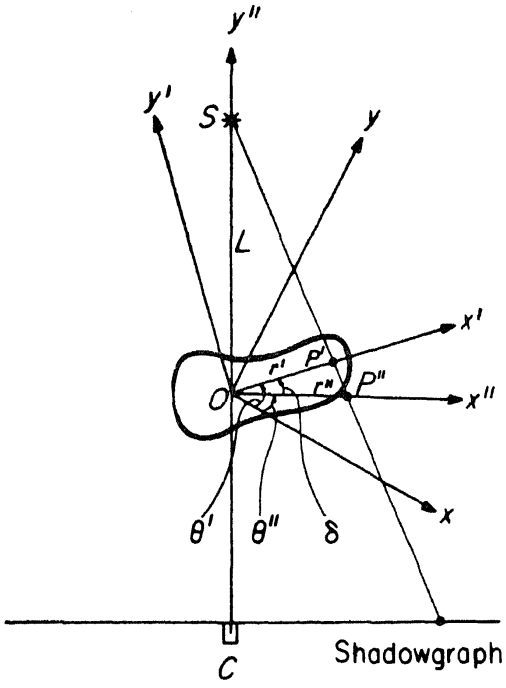


FIG. 4. Diagram illustrating the transformation of a divergent beam shadowgraph data into equivalent parallel beam data.

where

$$r'' = r' \sec \delta, \tag{20 a}$$

$$\theta'' = \theta - \delta, \tag{20 b}$$

and

$$\sin \delta = \frac{r'}{L}. \tag{20 c}$$

In practical problems, the relation $dr'' = \cdot \sec \delta \, dr'$ must also be used in converting from the divergent beam data to the equivalent parallel beam data.

Clearly, Eqs. (19) and (20) can be computerised to convert the divergent beam data by interpolation and unscrambling to obtain a set of functions $g(r'; \theta)$ at suitable intervals, which can be fed into Eq. (12) exactly as in the parallel beam case.

Alternatively, a recorder such as a counting device may be kept at C (Fig. 4) in the line SO, and both S and C could be translated together parallel to $Ox''$ to record directly the function $g(r''; \theta'')$. This function is then ready to be fed into Eq. (12), with $\theta''$ as the relevant angle variable. The only disadvantage in this technique is that mechanical motion is needed, while the data can be recorded electronically at fixed settings, if the unscrambling process is adopted.

V. *Test of the method by computer simulation of shadowgraphs.*—By making a computer simulation of the shadowgraphs, taken at 3° intervals for 0° to 180°, for the lamellar structure shown in Fig. 5 (*a*), the Fourier transformation and reconstruction was made by taking measurements of $g(r; \theta)$ at intervals of 0·1 cm and using only 25 orders of Fourier coefficients ($-12\,R_0$ to $+12\,R_0$, $R_0 = 0{\cdot}25$ cm$^{-1}$). The optical density of the reconstructed material is shown in Fig. 5 (*b*), showing that even with such rough data, the reconstruction is quite good. If "fast Fourier" methods are used, about 1,000 one-dimensional syntheses can be made in a second. The problems involved in accuracy of reproduction and resolution, in relation to the relative efficiencies of digital and analogue methods of Fourier summation, are under study.

References to some publications which also discuss three-dimensional reconstructions using Fourier transforms, but somewhat different from the treatment in this paper, may be obtained from a recent paper by Crowther *et al.*[6]

VI. *Autoradiography.*—In some methods of tumour detection, *e.g.*, in the brain, a radioactive isotope which concentrates in the tumour, such as $I^{131}$, is injected into the blood stream, and a "brain scan" is made by detecting the $\gamma$-radiation emitted by the isotope by a collimated scanner.[7] It is common to take the brain scan in two, or three, directions $\theta$ (Fig. 2 *b*), and make the diagnosis from these. Although the technique is slightly different from the recording of radiographic shadows (Fig. 2 *a*), it is

possible to derive formulae, involving Fourier transforms, of the type presented in this paper, in order to obtain a three-dimensional reconstruction of the tumour in the form of a function giving the emissive power per unit volume of the radiation, which may be taken to be proportional to the concentration of the radioactive isotope. The details are omitted, the main purpose here being only to indicate that, by using suitable mathematical techniques involving Fourier transformation and the use of large-scale computers, three-dimensional reconstruction can be made under a variety of situations of useful practical interest.

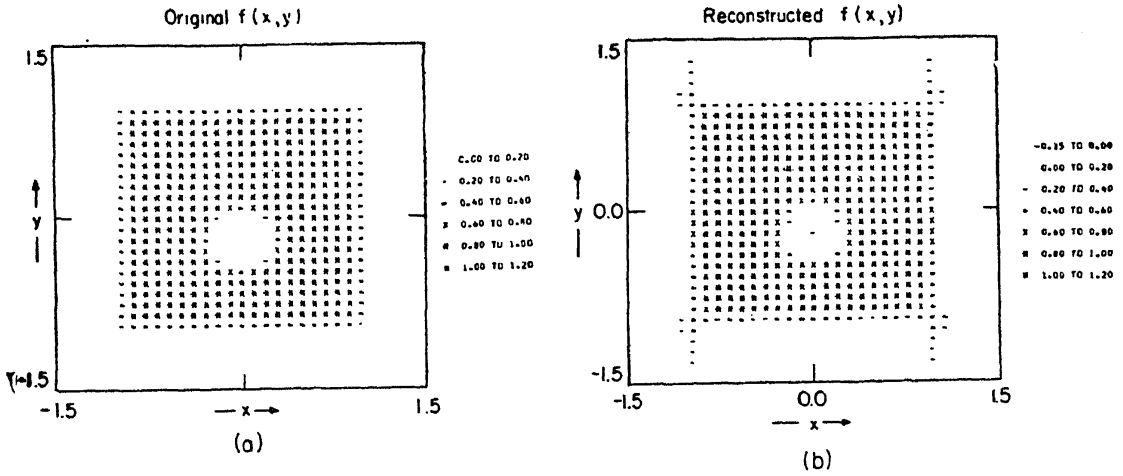


FIG. 5. Representation of a planar structure consisting of a square of uniform density (1·0) with a circular hole off-center. (*a*) Original structure, (*b*) Reconstructed structure from linear Fourier transforms calculated from computer-simulated shadowgraphs. The spikes observed at the corners of the square in the reconstruction are due to errors in the simulated shadowgraph, rather than due to the cutting off of the Fourier transform values.

VII. *Completing the missing data in electron microscopy.*—As mentioned in Section V, it is necessary to take shadowgraphs at regular intervals, over a complete half-rotation ($\theta = 0°$ to 180°), to obtain the complete Fourier transform in a plane. However, a rather recondite theorem in Fourier transform theory, due to Paley and Wiener,[8] makes it possible to obtain the values of the Fourier transform in missing regions of the ($R$, $\Phi$) -plane, if the function is completely known in the other regions. In one dimension, the theorem is equivalent to the statement that, if the object whose Fourier transform is obtained has finite size and mass [the exact condition is that the integral of $|f(x)|^2$ is finite], then the Fourier transform is analytic over its entire range. In the theory of complex variables, such an entire function has a Taylor expansion about every finite point.[9] Hence, if the function F (X) is known over a finite range $A < X < B$, then it can in principle be calculated over the entire range of X.

A direct extension of this theorem to two dimensions makes it possible to calculate F(X, Y) or F(R, $\Phi$) over the entire (X, Y)-plane, if it is known completely over a finite area, so that all its derivatives can be computed. The problem that remains is only one of practical computation using suitable methods of numerical analysis (which has not yet been solved).

However, the possibilities raised by the Paley-Wiener theorem are of great interest in electron microscopy, in which the stage holding the object may obstruct the electron beam over a finite range of $\theta$ values, so that, say, only data between $\theta = 30°$ to 150° are available for $g(r; \theta)$. Then, F(R, $\theta$) is also available only over this range. The data in the missing sectors can, in principle, be covered by using the method of analytic continuation.

## REFERENCES


1. Ramachandran, G. N. and Srinivasan, R. — *Fourier Methods in Crystallography*, Ed. M. J. Buerger, Wiley, New York, 1970.
2. Fernandez-Moran, H. .. *Abst. Seventh International Congress of Electron Microscopy*, Grenoble, 1970.
3. ——, Ohtsuki, M., Hafner, S. S. and Virgo, D. — *Proceedings of the Apollo II Lunar Science Conference*, 1970, **1**, 409–17.
4. Crewe, A. V. .. *Quart. Rev. Biophys.*, 1970, **3**, 137.
5. ——, Wall, J. and Langmore, J. — *Science*, 1970, **168**, 1338.
6. Crowther, R. A., Ames, L. A., Finch, J. T., DeRosier, D. J. and Klug, A. — *Nature*, 1970, **226**, 421.
7. Wang, Y. .. *Clinical Radioisotope Scanning*, Charles C. Thomas, Springfield, 1968, p. 65.
8. Paley, R. E. A. C. and Wiener, N. — *Fourier Transforms in the Complex Domain*, American Mathematical Society, New York, 1934, pp. 7, 12.
9. Fuchs, B. A. and Shabat, B. V. — *Functions of a Complex Variable*, Hindustan Publishing Corporation, Delhi, 1962, p. 267.